Available online at www.sciencedirect.com
SCIENCE DIRECT
Polymer 46 (2005) 9230–9242
polymer
www.elsevier.com/locate/polymer

Synthesis, thermal and optical properties of liquid crystalline terpolymers containing azobenzene and dye moieties

Raquel Giménez[a], Marta Millaruelo[a], Milagros Piñol[b], José Luis Serrano[a,*], Ana Viñuales[a], Regina Rosenhauer[c], Thomas Fischer[c], Joachim Stumpe[c]

[a]*Química Orgánica, Facultad de Ciencias-Instituto de Ciencia de Materiales de Aragón, Universidad de Zaragoza-CSIC, Pedro Cerbuna, 12, 50009 Zaragoza, Spain*
[b]*Química Orgánica, Escuela Politécnica Superior de Huesca-Instituto de Ciencia de Materiales de Aragón, Universidad de Zaragoza-CSIC, 22074 Huesca, Spain*
[c]*Fraunhofer Institute of Applied Polymer Research, Science Park Golm, 14476 Potsdam, Geiselbergstr. 69, Germany*

Received 11 April 2005; received in revised form 6 July 2005; accepted 12 July 2005
Available online 15 August 2005

Abstract

The synthesis, thermal properties and photochemical and photophysical studies of new azopolymers are described. These polymers contain three different types of monomer, each of which is mainly responsible for a particular function: A mesogenic benzanilide, a photochromic azobenzene and a dye unit (a benzoxazole, an anthracene or a stilbene derivative). This approach provides liquid crystalline terpolymers with different spectral properties and with the potential ability to be photoaligned by irradiation and thermotropic self-organization. The polymers have been prepared by random radical polymerisation of the corresponding methacrylate-fucntionalised units. All of the materials show good thermal stability and liquid crystalline behaviour, displaying smectic A or nematic mesophases. Optical properties of the polymers in solution display additive bands in the absorbance spectrum and luminescent properties in the emission region of the individual dye monomers. However, films of these polymers are not luminescent. A study of the absorption and redox properties of the dyes has been performed in order to evaluate the quenching process in the polymers.

Keywords: Liquid crystal polymer; Azobenzene; Terpolymer

1. Introduction

The search for improved optical devices based on optically anisotropic films [1,2] such as polarisers, retarders or photoluminescent films for liquid crystal displays or OLEDs requires new materials that give absorption or emission properties in different spectral regions, are stable under irradiation and easy to orient and process. In this context, we are interested in the design of polymers that combine all of these features by the preparation of liquid crystalline (LC) polymers containing azobenzene and different dyes. Polymers with azobenzene groups show the well-known photochromic effect, i.e. their absorption changes in a reversible way upon irradiation with light of different wavelengths due to the *E*/*Z* photoisomerisation of the azobenzene group. This effect generates optical anisotropy in films under irradiation with linearly polarised light, as the azobenzene groups become oriented perpendicular to the electric field of the incident light [3–5]. If the polymers are side-chain polymeric liquid crystals, the photoinduced order generated in the glassy state can be significantly amplified by annealing in the LC phase, which allows high order parameters to be reached with short irradiation times [6–10].

There are two main approaches for the molecular design of photochromic polymers, blending a polymeric matrix with dye molecules or copolymerisation. The second option gives polymers with covalently connected dye molecules and this approach has certain advantages over polymer-dye host–guest mixtures. For example, covalent linking avoids the major problem of phase separation and allows high concentrations of several different monomers without

* Corresponding author. Tel./fax: +34 976 761 209.
E-mail address: joseluis@unizar.es (J.L. Serrano).

0032-3861/$ - see front matter © 2005 Elsevier Ltd. All rights reserved.
doi:10.1016/j.polymer.2005.07.040

distortion of the LC properties of the matrix [11]. Indeed, this approach has proved successful with ternary chiral photochromic LC copolymers for optical data recording and storage [12].

In the case reported here we prepared the terpolymers $\mathbf{TP}_{blue}$, $\mathbf{TP}_{green}$ and $\mathbf{TP}_{red}$, which are side-chain polymers that consist of three different types of monomer, each of which is mainly responsible for a particular function (Scheme 1). These compounds all contain a mesogenic group (70 mol%) based on benzanilide ($\mathbf{M}_{am}$), which acts as the LC matrix, and a photochromic azobenzene unit ($\mathbf{M}_{azo}$) (15 mol%). The third monomer is a dye-based unit that will provide different optical properties in the material and this component was incorporated at a level of 15 mol%. In order to study absorption and emission properties, three different luminescent dyes were employed: A benzoxazole ($\mathbf{M}_{blue}$) that emits blue light, an anthracene ($\mathbf{M}_{green}$) that produces green light and a push–pull substituted stilbene emitting red light ($\mathbf{M}_{red}$). Dyes were chosen according to their emission properties, their possible asymmetric functionalisation for incorporation as side-chain monomers and their mesogenic or promesogenic rod-like shape.

It was not clear whether the three different monomers would act in an additive way in the terpolymer as different interactions may exist in the polymeric system. For this reason, a complete study of the optical properties of the terpolymers is presented. The model copolymer ($\mathbf{CP}_1$) that only contains the mesogenic and photochromic azo units was also prepared and investigated for comparison purposes. In addition, the photochemical stability and redox properties of the dyes were also investigated using non-reactive model compounds ($\mathbf{D}_{blue}$, $\mathbf{D}_{green}$ and $\mathbf{D}_{red}$).

2. Experimental

2.1. Synthesis of the monomers and model dyes

Monomers $\mathbf{M}_{am}$, $\mathbf{M}_{azo}$ and $\mathbf{M}_{red}$ were synthesised as reported in the literature [13–15]. With respect to the model dyes, $\mathbf{D}_{blue}$ was synthesised in an analogous way to $\mathbf{M}_{blue}$ and the synthesis of $\mathbf{D}_{green}$ has recently been reported [16]. $\mathbf{D}_{red}$ is a commercially available dye.

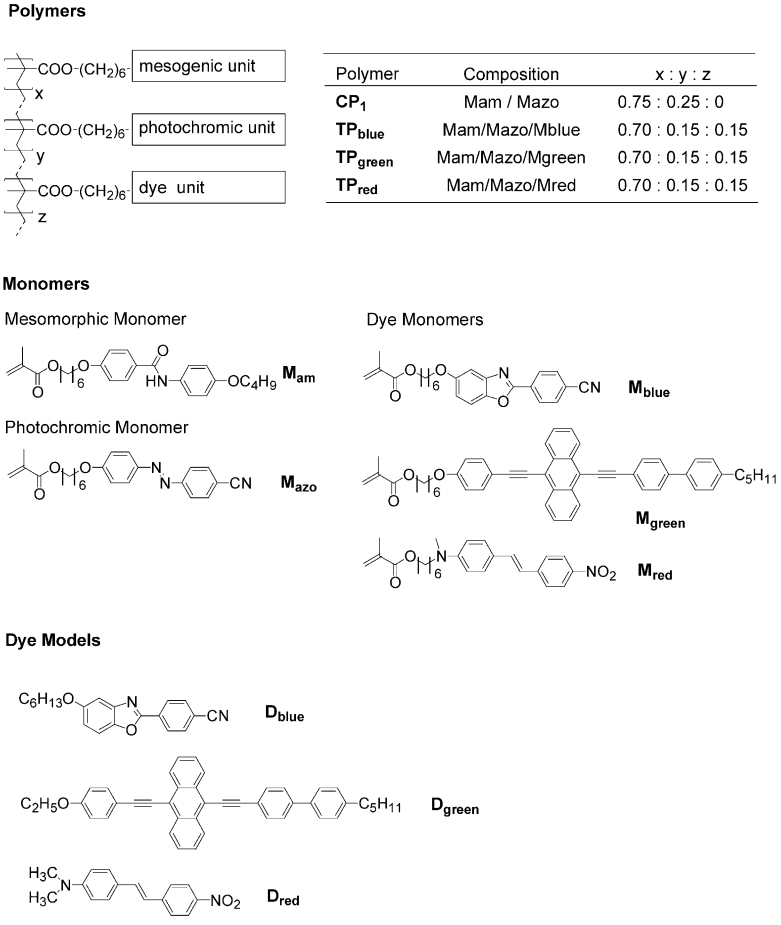

Polymer	Composition	x : y : z
$\mathbf{CP}_1$	Mam / Mazo	0.75 : 0.25 : 0
$\mathbf{TP}_{blue}$	Mam/Mazo/Mblue	0.70 : 0.15 : 0.15
$\mathbf{TP}_{green}$	Mam/Mazo/Mgreen	0.70 : 0.15 : 0.15
$\mathbf{TP}_{red}$	Mam/Mazo/Mred	0.70 : 0.15 : 0.15

Scheme 1. Chemical structures of the polymers, monomers and model dyes.

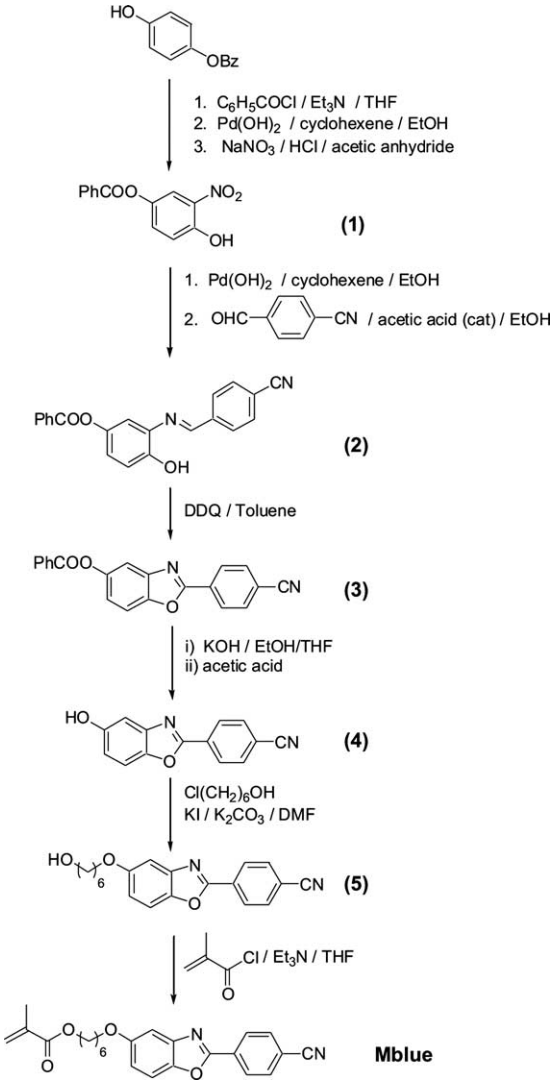

Scheme 2. Synthesis of the monomer $\mathbf{M}_{blue}$.

2.1.1. Synthesis of the benzoxazole monomer (M_{blue}) (Scheme 2)

*2.1.1.1. Synthesis of 4-hydroxy-3-nitrophenyl benzoate (**1**).* Benzoyl chloride (7 mL) was added dropwise to a solution of 4-benzyloxyphenol (10.0 g, 0.05 mol) and triethylamine (6.1 g, 0.06 mol) in dry THF at room temperature. The resulting mixture was stirred for 30 min and the resulting precipitate was filtered off. The solution was washed with saturated Na_2CO_3 solution (2×100 mL) and water (3×100 mL), dried over $MgSO_4$, and evaporated to dryness to yield 4-benzyloxyphenyl benzoate as a white solid (13.4 g, 88% yield). $Pd(OH)_2$ on carbon (3.9 g) was gradually added under argon to a boiling mixture of 4-benzyloxyphenyl benzoate (13.0 g, 0.04 mol) in absolute ethanol (170 mL) and cyclohexene (85 mL). After 2 h the reaction was cooled down to room temperature, filtered through a pad of Celite® and evaporated under vacuum to give 4-hydroxyphenyl benzoate as a white solid (8.5 g, 99% yield). A solution of 4-hydroxyphenyl benzoate (8.5 g, 0.04 mmol) in dichloromethane (CH_2Cl_2) (94 mL) and diethyl ether (189 mL) was added to a stirred solution of $NaNO_3$ (3.4 g, 0.04 mol) in concentrated HCl (35.4 mL) and H_2O (47 mL) at room temperature. Acetic anhydride (0.6 mL) was added and the reaction mixture was stirred for 4 h. The organic phase was separated and the aqueous layer extracted with diethyl ether (2×60 mL). The combined organic layers were dried over $MgSO_4$ and the solvent removed under reduced pressure. The resulting solid was recrystallised from ethanol to give **1** as a spongy yellow solid (7.8 g, 76% yield). ^{1}H NMR [300 MHz, $CDCl_3$, δ (ppm)]: 10.50 (s, 1H), 8.17 (dd, J= 8.4, 1.3 Hz, 2H), 7.99 (d, J=2.7 Hz, 1H), 7.65 (m, 1H), 7.51 (dd, J=8.4, 7.5 Hz, 2H), 7.47 (dd, J=9.0, J=2.7 Hz, 1H), 7.21 (d, J=9.0 Hz, 1H). IR (Nujol, cm^{-1}) υ:=3284, 1738, 1536, 1328.

*2.1.1.2. Synthesis of 3-(4′-cyanophenylbenzylideneamino)-4-hydroxyphenyl benzoate (**2**).* Compound **1** was dissolved in absolute ethanol and cyclohexene (about 45 mL/g of the nitroderivative) with stirring. The reaction mixture was heated under reflux and $Pd(OH)_2$ on carbon (about 30% of nitroderivative weight) was added under argon. The mixture was protected from light and the progress of the reaction followed by thin layer chromatography. After consumption of the starting material (about 4 h), the reaction was cooled down to room temperature and filtered through a pad of Celite®. The solvent was removed under vacuum to give the *ortho*-aminophenol as an oil. This oil, without further purification, was dissolved in absolute ethanol and added under argon to a solution of 4-cyanobenzaldehyde in absolute ethanol. The mixture was heated under reflux with acetic acid (catalytic amount) and stirred for 12 h. The resulting solution was concentrated and the residue recrystallised from absolute ethanol to give the corresponding imine **2** (70% yield). ^{1}H NMR [300 MHz, $CDCl_3$, δ (ppm)]: 8.69 (s, 1H), 8.18 (d, J=7.5 Hz, 2H), 7.99 (d, J= 8.2 Hz, 2H), 7.76 (d, J=8.2 Hz, 2H), 7.63 (m, 1H), 7.50 (t, J=7.6 Hz, 2H), 7.25–7.23 (m, 2H), 7.10–7.04 (m, 2H). IR (Nujol, cm^{-1}) υ:=3358, 2222, 1732, 1626.

*2.1.1.3. Synthesis of 5-benzoyloxy-2-(4′-cyanophenyl)benzoxazole (**3**).* 2,3-Dichloro-5,6-dicyano-1,4-benzoquinone (DDQ) (2.7 g, 12.00 mmol) was added gradually to a solution of imine **2** (6.00 mmol) in toluene (200 mL) (previously dried over 4 Å molecular sieves) and the mixture was heated under reflux for 2 h. The reaction was cooled to room temperature and saturated aqueous $NaHCO_3$ (200 mL) was added. The mixture was extracted with CH_2Cl_2 (4×100 mL) and the combined organic layers washed with water (4×100 mL) and dried over $MgSO_4$. The solution was concentrated under vacuum and a large volume of hexane was added to precipitate the desired compound, which was filtered off and purified by flash column chromatography on silica gel using CH_2Cl_2 as eluent (77% yield). ^{1}H NMR [300 MHz, $CDCl_3$, δ (ppm)]:

8.34 (d, $J=8.7$ Hz, 2H), 8.22 (d, $J=7.1$ Hz, 2H), 7.81 (d, $J=8.7$ Hz, 2H), 7.65–7.61 (m, 3H), 7.52 (m, 2H), 7.25 (dd, $J=8.8$, 2.4 Hz, 1H). IR (Nujol, cm^{-1}) υ: = 2229, 1731, 1614.

*2.1.1.4. Synthesis of 2-(4′-cyanophenyl)-5-hydroxybenzoxazole (**4**).* A solution of KOH (200 mg) in water (5 mL) was added dropwise to a solution of benzoxazole **3** (1.2 g, 3.67 mmol) in THF (100 mL) and 96% ethanol (25 mL) at room temperature. The mixture was stirred for 2 h and a large volume of water was added. The resulting mixture was neutralized with acetic acid and the THF was removed under reduced pressure in order to precipitate the target compound (**4**). The product was filtered off and dried at 45 °C for 48 h under vacuum (801 mg, 93%). ^{1}H NMR [300 MHz, $CDCl_3$, δ (ppm)]: 8.31 (d, $J=8.4$ Hz, 2H), 7.79 (d, $J=8.0$ Hz, 2H), 7.45 (d, $J=8.8$ Hz, 1H), 7.22 (d, $J=2.6$ Hz, 1H), 6.92 (dd, $J=9.3$, 2.5 Hz, 1H), 4.92 (s, 1H). IR (Nujol, cm^{-1}) υ: = 3389, 2237, 1615.

*2.1.1.5. Synthesis of 2-(4′-cyanophenyl)-5-(6′-hydroxyhexyl-1′-oxy)benzoxazole (**5**).* A mixture of compound **4** (0.750 g, 3.2 mmol), 6-chloro-1-hexanol (0.481 g, 3.52 mmol), K_2CO_3 (0.663 g, 4.8 mmol) and KI (0.106 g, 0.64 mmol) in DMF (100 mL) was heated under reflux for 4 h. The reaction mixture was cooled to room temperature, water was added and the product extracted with hexane/ethyl acetate (1:2). The combined organic extracts were washed with water, dried over $MgSO_4$ and evaporated to dryness. The crude product was recrystallised from hexane/dichloromethane to yield the required product (0.935 g, 87% yield). ^{1}H NMR [300 MHz, $CDCl_3$, δ (ppm)]: 8.30 (d, $J=8.2$ Hz, 2H), 7.78 (d, 8.1 Hz, 2H), 7.46 (d, $J=9.0$ Hz, 1H), 7.23 (d, $J=2.6$ Hz, 1H), 6.99 (dd, $J=9.0$, 2.7 Hz, 1H), 4.00 (t, $J=6.2$ Hz, 1H), 3.65 (t, $J=6.4$ Hz, 2H), 1.85–1.80 (m, 2H), 1.63–1.47 (m, 6H). IR (Nujol, cm^{-1}) υ: = 3415, 3342, 2222, 1616.

2.1.1.6. Synthesis of 6-[2-(4′-cyanophenyl)benzoxazol-5-yloxy]hexyl methacrylate M_{blue}. Methacryloyl chloride (0.233 g, 2.23 mmol) was added to a solution of benzoxazole (**5**) (0.500 g, 1.49 mmol), triethylamine (0.300 g, 2.96 mmol) and 2,6-di-*tert*-butyl-4-methylphenol (3 mg) in THF (50 mL) at 50 °C under argon. After 24 h, 10% aqueous NH_4Cl (50 mL) was added. The mixture was extracted with CH_2Cl_2 and the combined organic extracts washed with water, dried over $MgSO_4$ and evaporated to dryness. The crude product was recrystallised from ethanol to yield the final benzoxazole monomer (0.816 g, 87% yield). ^{1}H NMR [300 MHz, $CDCl_3$, δ (ppm)]: 8.31 (d, $J=8.6$ Hz, 2H), 7.79 (d, 8.6 Hz, 2H), 7.46 (d, $J=9.0$ Hz, 1H), 7.23 (d, $J=2.6$ Hz, 1H), 6.98 (dd, $J=8.9$, 2.6 Hz, 1H), 6.08 (s, 1H), 5.53 (s, 1H), 4.15 (t, $J=6.6$ Hz, 2H); 4.00 (t, $J=6.2$ Hz, 2H), 1.92 (m, 3H), 1.85–1.66 (m, 4H), 1.46–1.51 (m, 4H). ^{13}C NMR [300 MHz, $CDCl_3$, δ (ppm)]: 167.5, 161.5, 157.2, 145.5, 142.7, 136.5, 132.6, 131.2, 127.8, 125.2, 118.2, 115.6, 114.5, 111.0, 103.7, 68.6, 64.6, 29.1, 28.5, 25.8, 25.7, 25.6, 18.3. IR (Nujol, cm^{-1}) υ: = 2224, 1720, 1634, 1619. Anal. Calcd for $C_{24}H_{24}N_2O_5$: C, 71.32%; H, 5.94%; N, 6.93%. Found: C, 71.24%; H, 5.71%; N, 6.95%.

2.1.2. Synthesis of the anthracene monomer (M_{green}) (Scheme 3)

*2.1.2.1. Synthesis of 4-ethynyl-4-pentylbiphenyl (**6**).* Dry diisopropylamine (3 mL) and trimethylsilylacetylene (3 mL, 21.2 mmol) were added dropwise to a Schlenk tube charged with 4-pentyl-4′-bromophenyl (5 g, 16.5 mmol), CuI (63 mg, 0.33 mmol) and dichlorobis(triphenylphosphine)palladium(II) (116 mg, 0.16 mmol) in dry toluene (50 mL). The mixture was stirred at 70 °C for 2 days under an Ar atmosphere. The diisopropylamine was evaporated under vacuum and the toluene suspension filtered through a pad of silica gel. The solvent was evaporated in a rotary evaporator, the residue taken into THF (80 mL) and methanol (5 mL) and a 20% aqueous KOH (5 mL) was added. The reaction mixture was stirred overnight at room temperature. The mixture was filtered and the resulting solution evaporated to dryness. The residue was dissolved in hexanes (50 mL), washed with water, dried over $MgSO_4$ and evaporated to dryness. The crude product was purified by flash column chromatography on silica gel using hexanes as eluent to yield compound **6** as a white solid (63% yield). ^{1}H NMR [300 MHz, $CDCl_3$, δ (ppm)]: 7.54 (s, 4H), 7.49 (d, $J=8.0$ Hz, 2H), 7.25 (d, $J=8.3$ Hz, 2H), 3.11 (s, 1H), 2.63 (t, $J=6.5$ Hz, 2H), 1.66–1.61 (m, 2H), 1.36–1.31 (m, 4H), 0.89 (t, $J=6.8$ Hz, 3H). IR (Nujol, cm^{-1}) υ: = 3275, 2108, 1491, 835, 813.

*2.1.2.2. Synthesis of 9-bromo-10-(4′-pentylbiphenyl-4-ylethynyl)anthracene (**7**).* A solution of compound **6** (4.50 g, 18.14 mmol) in toluene (30 mL) was added dropwise to a Schlenk tube charged with 9,10-dibromoanthracene (5.54 g, 16.5 mmol), CuI (63 mg, 0.33 mmol), dichlorobis(triphenylphosphine)palladium(II) (116 mg, 0.16 mmol), dry toluene (300 mL) and dry diisopropylamine (3.5 mL) at 70 °C. The addition was carried out using an addition funnel over 12 h. The reaction mixture was stirred at this temperature for 1 day under an Ar atmosphere. The solvent was evaporated to dryness and the crude product purified twice by flash column chromatography on silica gel using firstly hexane and secondly hexane/dichloromethane (10:1) as eluent to yield the desired compound as a yellow solid (33% yield). ^{1}H NMR [300 MHz, $CDCl_3$, δ (ppm)]: 8.70–8.74 (m, 2H), 8.59–8.56 (m, 2H), 7.82 (d, $J=8.0$ Hz, 2H), 7.70–7.57 (m, 8H), 7.30 (d, $J=8.0$ Hz, 2H), 2.67 (t, $J=7.5$ Hz, 2H), 1.67–1.65 (m, 2H), 1.39–1.25 (m, 4H), 0.89 (t, $J=6.6$ Hz, 3H). IR (Nujol, cm^{-1}) υ: = 1492, 753.

*2.1.2.3. Synthesis of 6-(4′-iodophenyloxy)hexan-1-ol (**8**).* A mixture of 4-iodophenol (6.5 g, 29.5 mmol), 6-chlorohexanol (4.43 g, 32.4 mmol), K_2CO_3 (6.1 g, 44.25 mmol)

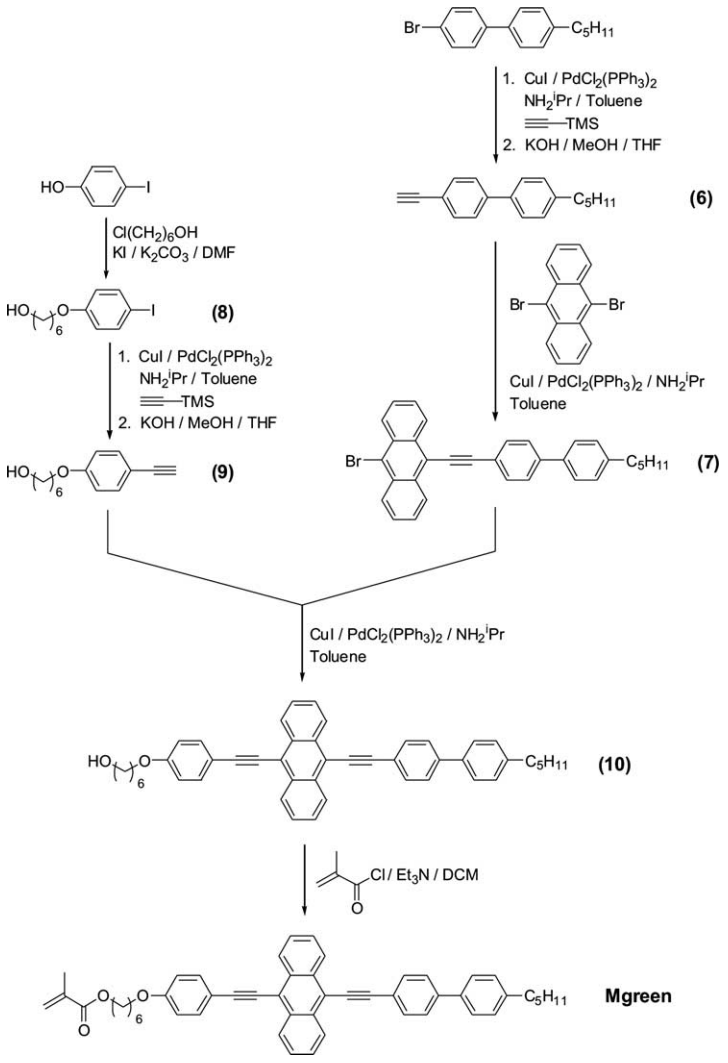

Scheme 3. Synthesis of monomer $\mathbf{M}_{green}$.

and KI (0.98 g, 5.9 mmol) in dry DMF was heated at 120 °C for 5 h. The reaction mixture was cooled to room temperature and water (200 mL) and hexane/ethyl acetate (100 mL) were added. The organic layer was separated, washed with water (100 mL), dried over $MgSO_4$ and evaporated to dryness. The product was purified by recrystallisation from hexane (86% yield). ^{1}H NMR [300 MHz, $CDCl_3$, δ (ppm)]: 7.52 (d, J= 8.8 Hz, 2H), 6.65 (d, J=8.8 Hz, 2H), 3.96 (t, J=6.5 Hz, 2H), 3.66 (t, J=6.5 Hz, 2H), 1.80–1.75 (m, 2H), 1.65–1.50 (m, 2H), 1.50–1.38 (m, 4H). IR (Nujol, cm^{-1}) υ: =3295, 1588, 1569, 1249.

*2.1.2.4. Synthesis of 6-(4′-ethynylphenyloxy)hexan-1-ol (**9**).* This compound was prepared following the same procedure as for compound **6** (46% yield). ^{1}H NMR [300 MHz, $CDCl_3$, δ (ppm)]: 7.42 (d, J=8.8 Hz, 2H), 6.82 (d, J= 8.8 Hz, 2H), 3.95 (t, J=6.5 Hz, 2H), 3.66 (t, J=6.5 Hz, 2H), 2.99 (s, 1H), 1.84–1.75 (m, 2H), 1.64–1.54 (m, 2H), 1.54–1.40 (m, 4H). IR (Nujol, cm^{-1}) υ: =3304–3214, 2099, 1602, 1567, 1503, 1248.

*2.1.2.5. Synthesis of 6-{4-[10-(4′-pentylbiphenyl-4-ylethynyl)anthracen-9-ylethynyl]phenoxy}hexan-1-ol (**10**).* A solution of compound **9** (381 mg, 1.7 mmol) in dry toluene (30 mL) was added dropwise to a Schlenk tube charged with compound **7** (800 mg, 1.6 mmol), CuI (6 mg, 0.032 mmol), dichlorobis(triphenylphosphine)palladium(II) (11 mg, 0.016 mmol), dry toluene (30 mL) and dry diisopropylamine (0.3 mL) at 70 °C. The reaction mixture was heated at 70 °C for 3 day, filtered through a pad of Celite® and evaporated to dryness. The residue was purified by flash column chromatography on silica gel using eluents of increasing polarity:hexane/dichloromethane (3:1), CH_2Cl_2 and CH_2Cl_2/ethyl acetate (10:1). The pure product was obtained as a dark yellow solid (67% yield). ^{1}H NMR [300 MHz, $CDCl_3$, δ (ppm)]: 8.72–8.64 (m, 4H), 7.81 (d, J=8.5 Hz, 2H), 7.70–7.54 (m, 10H), 7.28 (d, J=8.5 Hz, 2H), 6.95 (d, J=8.5 Hz, 2H), 4.02 (t, J=6.6 Hz, 2H), 3.67 (t, J=6.6 Hz, 2H), 2.65 (t, J=7.5 Hz, 2H), 1.83–1.81 (m, 2H), 1.66–1.60 (m, 4H), 1.50–1.45 (m, 2H), 1.37–1.23 (m, 6H), 0.92

(t, $J=6.0$ Hz, 3H). IR (KBr, cm^{-1}) υ: = 3480–3323, 2193, 1508, 1242, 764.

*2.1.2.6. Synthesis of 6-{4-[10-(4′-pentylbiphenyl-4-ylethynyl)anthracen-9-ylethynyl]phenoxy}hexyl methacrylate (**M**$_{green}$).* A mixture of compound **10** (900 mg, 1.4 mmol), methacryloyl chloride (0.27 mL, 2.8 mmol), triethylamine (0.59 mL, 4.2 mmol) and a catalytic amount of a thermal inhibitor (2,6-di-*tert*-butyl-4-methylphenol) in dry CH_2Cl_2 (50 mL) was stirred and heated under reflux for 5 h under an Ar atmosphere. The solvent was evaporated and the crude product purified by flash column chromatography using CH_2Cl_2 as the eluent. The product was further purified by recrystallisation from hexane to yield a golden yellow solid (58% yield). UV–vis (THF): 275, 326, 453, 476 nm. Emission (THF): 492, 525 nm (exc 451 or 474 nm). ^{1}H NMR [300 MHz, $CDCl_3$, δ (ppm)]: 8.71–8.68 (m, 4H), 7.82 (d, $J=8.4$ Hz, 2H), 7.71–7.56 (m, 10H), 7.28 (d, $J=8.4$ Hz, 2H), 6.95 (d, $J=8.4$ Hz, 2H), 6.10 (m, 1H), 5.54 (m, 1H), 4.16 (t, $J=6.6$ Hz, 2H), 4.02 (t, $J=6.6$ Hz, 2H), 2.65 (t, $J=7.5$ Hz, 2H), 1.94 (s, 3H), 1.83–1.81 (m, 2H), 1.75–1.65 (m, 4H), 1.54–1.37 (m, 4H), 1.37–1.34 (m, 4H), 0.90 (t, $J=6.6$ Hz, 3H). ^{1}H NMR [300 MHz, $CDCl_3$, δ (ppm)]: 160.6, 159.5, 156.0, 142.7, 141.3, 137.5, 137.4, 136.4, 133.2, 133.1, 132.1, 132.0, 131.8, 128.9, 127.2, 126.7, 125.1, 121.9, 118.9, 115.3, 114.7, 102.3, 87.1, 67.9, 38.1, 38.0, 35.5, 31.4, 29.0, 25.7, 25.6, 22.5, 18.2, 13.9. IR (KBr, cm^{-1}) υ: = 3054, 2194, 1717, 1636, 1601, 1509, 1248. Anal. Calcd for $C_{51}H_{48}O_3$ (%): C, 86.40; H, 6.82. Found: C, 86.54%; H, 6.73%.

2.2. Synthesis and characterisation of the polymers

2.2.1. Polymerisation procedure

The monomeric mixture was dissolved in freshly distilled *N*,*N*-dimethylformamide (DMF) (approximately 10% w/v) under an argon atmosphere in a Schlenk tube. The sample was degassed by several vacuum/argon cycles, the solution was heated to 70 °C and azobis(isobutyronitrile) (AIBN) (1% weight ratio) was added. The solution was stirred at this temperature for at least 48 h and the progress of the polymerisation was monitored by thin layer chromatography (TLC). In the case of the terpolymers, a significant proportion of the monomers was still unreacted and so additional AIBN (1% weight ratio) was added every 24 h. The polymer was precipitated by pouring the reaction mixture into cold 96% ethanol and the product was filtered off. Purification was carried out by dissolving the polymer in dichloromethane and precipitating it in ethanol or hexane until complete removal of any residual unreacted monomers. The final product was dried under vacuum at 40 °C for 24 h.

2.2.2. Physical characterisation of **CP**$_1$

Orangey solid (48% yield). ^{1}H NMR [300 MHz, $CDCl_3$, δ (ppm)]: 8.45, 7.82, 7.68, 7.45, 6.90, 6.73, 3.83, 1.80–1.20, 0.89. IR (Nujol, cm^{-1}) υ: = 2226, 1725, 1645, 1603, 1510, 1247. Anal. Found (Calcd): %C, 71.30 (71.28); %H, 7.51 (7.49); %N, 4.68 (4.70). GPC (THF) M_w, 27,000; M_n, 18, 000; M_w/M_n: 1.5.

2.2.3. Physical characterisation of **TP**$_{blue}$

White solid (45% yield). ^{1}H NMR [300 MHz, $CDCl_3$, δ (ppm)]: 8.27, 8.00–7.60, 7.48, 6.82, 3.93, 1.90–0.90. IR (Nujol, cm^{-1}) υ: = 2226, 1725, 1645, 1606, 1511, 1248 Anal. Found (Calcd): %C, 70.20 (71.34); %H, 7.08 (7.36); %N, 5.01 (4.65). GPC (THF) M_w, 6000; M_n, 3300; M_w/M_n: 1.8.

2.2.4. Physical characterisation of **TP**$_{green}$

Yellow solid (37% yield). ^{1}H NMR [300 MHz, $CDCl_3$, δ (ppm)]: 8.65, 7.90–7.30, 7.30–7.10, 7.00–6.65, 3.91, 2.65, 1.91–1.23, 0.95. IR (Nujol, cm^{-1}) υ: = 3311, 2225, 1726, 1643, 1605, 1504, 1246. Anal. Found (Calcd): %C, 73.29 (74.66); %H, 7.08 (7.42); %N, 3.77 (3.44). GPC (THF) M_w, 7300; M_n, 5500; M_w/M_n: 1.3.

2.2.5. Physical characterisation of **TP**$_{red}$

Red solid (70% yield). ^{1}H NMR [300 MHz, $CDCl_3$, δ (ppm)]: 8.12, 7.90–7.75, 7.50, 6.84, 3.93, 3.31, 2.95, 1.95–0.95. IR (Nujol, cm^{-1}) υ: = 2224, 1723, 1643, 1604, 1580, 1508, 1242. Anal. Found (Calcd): %C, 70.18 (71.31); %H, 7.02 (7.52); %N, 4.92 (4.62). GPC (THF) M_w, 4800; M_n, 3200; M_w/M_n: 1.5.

2.3. Techniques for the characterisation of the polymers

Elemental analysis was performed with a Perkin–Elmer 240C microanalyzer. IR spectra were measured on a ATI-Mattson Genesis Series FTIR from Nujol mulls between NaCl disks. ^{1}H NMR spectra were recorded on a Varian Unity 300 spectrometer operating at 300 MHz. Gel permeation chromatography (GPC) was carried out on a Waters liquid chromatography system equipped with 600E multisolvent delivery system and a 996 photodiode array detector, using a combination of two Ultrastyragel® columns with pore sizes of 500 and 10^4 Å, THF as the mobile phase at 0.8 mL/min flow rate and calibration using polystyrene standards.

Mesogenic behaviour and transition temperatures were determined using an Olympus BH-2 polarising microscope equipped with a Linkam THMS hot-stage central processor and a CS196 cooling system. Differential scanning calorimetry (DSC) was performed using a DSC 2910 from TA Instruments with samples sealed in aluminum pans and a scanning rate of 10 °C/min under a nitrogen atmosphere. Temperatures were read at the maximum of the peak after prior heating of the sample to the isotropic liquid and cooling to 0 °C. Thermogravimetric analysis (TGA) was performed using a TA Instruments STD 2960 simultaneous TGA-DTA at a rate of 10 °C/min under a nitrogen atmosphere. TGA data are given as the onset of the

decomposition curve. In addition, the first derivative of the decomposition curve (DTGA) was read.

Optical absorption spectra in THF solution were recorded with an UV–vis spectrometer UV4-200 from ATI-Unicam. Luminescence measurements in THF solution were performed using a Perkin–Elmer LS50B spectrofluorimeter.

2.4. Photophysical and photochemical investigations

UV–vis absorption spectra were obtained using a Perkin–Elmer Lambda 2 spectrophotometer. Photoluminescence of the films was measured using a set-up with a linear arrangement of the following components: 100 W mercury lamp, cut-off filters, and Tidas diode fluorimeter (J&M). An integration time of 150 ms was used for the detection.

Films were spin-coated on silica glass substrates at 2000 rpm and an acceleration 700 rpm/s for 30 s using a Karl Suess CT 60 spin-coater.

The photochemical stability of the dyes was investigated using films of the non-reactive dyes ($\mathbf{D}_{blue}$, $\mathbf{D}_{green}$ and $\mathbf{D}_{red}$) in PMMA (0.1 mol of the dye per kilogram of PMMA). The films were spin coated from a solution containing 10 μmol of the corresponding dye and 1 mL of 10^{-4} M PMMA in THF. The photostability of the dyes was evaluated from the changes in their absorbance under irradiation. The benzoxazole ($\mathbf{D}_{blue}$) was irradiated with non-polarised light from a 100 W mercury lamp using an interference filter at 365 nm (34 mW/cm^2) while the stilbene ($\mathbf{D}_{red}$) and the anthracene ($\mathbf{D}_{green}$) derivatives were irradiated at 436 nm (22 mW/cm^2). The change of absorbance at the maximum was evaluated in terms of its dependence on the exposure time. The photostability is defined by the absorbed energy that causes a degradation corresponding to a 10% decrease in the dye absorbance. The absorbed energy E_{abs} was calculated from the power density of the incident light P, the irradiation time t and the mean absorbance A_{mean} between the start and the end of each irradiation interval (Eq. (1)) [17].

$$E_{abs} = tP(1 - 10^{-A_{mean}}) \quad (1)$$

It was assumed that the photoproducts do not absorb at the testing wavelength due to conversion to less-conjugated systems.

Emission properties of the terpolymers ($\mathbf{TP}_{blue}$, $\mathbf{TP}_{green}$ and $\mathbf{TP}_{red}$) were determined both in solution and in thin films. Films were spin-coated from a 0.15 M solution in $CHCl_3$ where the concentration was calculated on the basis of the polymer repeating unit. Excitation wavelengths were 335, 436 and 450 nm, depending on the dye absorption. Emission properties were also measured and compared to those determined for blends of the copolymer $\mathbf{CP}_1$ and the dyes ($\mathbf{D}_{blue}$, $\mathbf{D}_{green}$ or $\mathbf{D}_{red}$). Films were prepared by spin-coating using a solution containing 16 wt% of the dye and 84 wt% of the copolymer $\mathbf{CP}_1$. In all cases quenching of the emission was observed. The quenching efficiency was determined dividing the emission intensity of a terpolymer by the emission intensity of the related dye-containing PMMA film, using comparable absorption values at the excitation wavelength.

Quenching of the fluorescence for the benzoxazole dye was investigated in terms of its dependence on the azobenzene concentration. Mixtures of $\mathbf{D}_{blue}$ and $\mathbf{CP}_1$ were prepared in THF with the concentration of $\mathbf{D}_{blue}$ varied from 0.25 to 5×10^{-4} M and the concentration of $\mathbf{CP}_1$ from 4.75×10^{-4} to 0 M, resulting in a final concentration of 5×10^{-4} M.

In all the quenching experiments, the thickness of the cuvette was varied in such a way that the absorbance of the dyes were always the same.

2.5. Cyclic voltammetry

Cyclic voltammetry experiments in solution were performed using an EcoChemie Instrument. A three-electrode cell was used. The working electrode was a graphite electrode, a platinum wire was used as counter electrode and a $Hg/HgCl_2$ electrode was used as a reference. The redox properties were investigated in THF or dichloromethane solutions containing tetrabutylammonium hexafluorophosphate (0.1 M) as supporting electrolyte. The solutions were purged with argon. Cyclic voltammograms were obtained at room temperature with scan rates of 0.05 V/s.

3. Results and discussion

3.1. Synthesis, characterisation and optical properties of the monomers

The polymers were prepared by radical polymerisation in solution of the different terminal methacrylate monomers, the chemical structures of which are shown in Scheme 1. The benzanilide ($\mathbf{M}_{am}$) and the azobenzene ($\mathbf{M}_{azo}$) methacrylates were prepared as previously reported [13,14]. The stilbene monomer ($\mathbf{M}_{red}$) was obtained using the method described by Robello [15]. In all cases, the characterisation data are consistent with those in the literature.

The benzoxazole monomer ($\mathbf{M}_{blue}$) was prepared as shown in Scheme 2. The *ortho*-nitrophenol (**1**) was reduced to the corresponding *ortho*-aminophenol using palladium (II) hydroxide and cyclohexene and this was condensed with 4-cyanobenzaldehyde to yield the imine (**2**). Oxidative cyclization of the imine with DDQ yielded 2-(4′-cyanophenyl)-5-hydroxybenzoxazole (**4**). Finally, the spacer and the methacrylate moiety were introduced by successive alkylation and esterification steps.

The non-symmetrically substituted anthracene comonomer ($\mathbf{M}_{green}$) was obtained by the synthetic pathway represented in Scheme 3, which consists of two sequential

Sonogashira cross-coupling reactions using 9,10-dibromoanthracene. The first coupling reaction was the key step and this was carried out in a dilute reaction medium to minimise the formation of the undesired disubstituted product. Nevertheless, subsequent separation of the product by column chromatography was required.

For both comonomers, $\mathbf{M}_{blue}$ and $\mathbf{M}_{green}$, the methacryloyl unit was incorporated in the last step of the reaction sequences in order to avoid undesired reaction of this reactive unit in the intermediate steps.

The thermal properties of the monomers were investigated by optical microscopy and DSC and the results are gathered in Table 1. Only the anthracene monomer $\mathbf{M}_{green}$ showed liquid crystalline behaviour and this gave a stable nematic phase between 120 and 220 °C.

The optical properties of the monomers were determined from THF solutions. The spectra are compared in Fig. 1(a). It can be seen that all the compounds show strong absorption bands in the UV region due to their conjugated aromatic cores. $\mathbf{M}_{am}$ shows a band centered at 280 nm and this does not have significant fluorescent emission [18]. $\mathbf{M}_{azo}$ displays an absorption band at 364 nm related to the π–π* transition and a weak absorption band about 450 nm corresponding to the n–π* transition.

$\mathbf{M}_{blue}$ has two absorption bands at 296 and 336 nm and, on excitation of the second one, exhibits blue emission. The absorption spectrum of $\mathbf{M}_{green}$ exhibits two intense peaks at around 455 and 474 nm. In the emission spectrum two peaks can be observed, a sharp one in the blue–green region (495 nm) and a weaker one in the green region (525 nm), and these make the compound show an intense green fluorescence. $\mathbf{M}_{red}$ displays an absorption band at 444 nm and, upon excitation at this wavelength, $\mathbf{M}_{red}$ shows an orange–red emission at 605 nm. It should be noted that, in contrast to $\mathbf{M}_{blue}$ and $\mathbf{M}_{green}$, $\mathbf{M}_{red}$ shows a weak fluorescence caused by the presence of the nitro group [19].

Table 1
Thermal and optical properties of monomers

Monomer	Thermal transitions[a]	Optical properties[b]		
		λ_{abs} (nm)	ε (cm^{-1} M^{-1})	λ_{em} (nm)
$\mathbf{M}_{am}$	Cr 134 I	280	19,646	
$\mathbf{M}_{azo}$	Cr 71 I	364	22,320	
$\mathbf{M}_{blue}$	Cr 86 I	296, 336	13,769, 16,461	443
$\mathbf{M}_{green}$	Cr 120 N 220 I	455, 474	43,652, 41,687	493, 524
$\mathbf{M}_{red}$	Cr 90 I	444	11,545	605

[a] Temperatures are given in °C, Cr, crystal phase; I, isotropic liquid; N, nematic phase.

[b] Optical properties determined in THF solution. UV–vis absorption was measured in approximately 10^{-5} M. Emission was determined from approximately 10^{-7} M solutions.

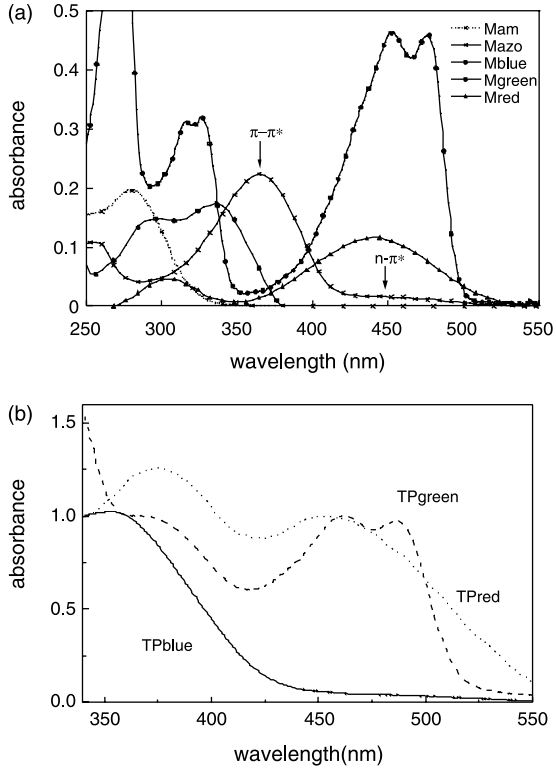

Fig. 1. Absorbance spectra: (a) Absorbance spectra of monomers $\mathbf{M}_{am}$ (dash-crossed line), $\mathbf{M}_{azo}$ (solid-crossed line), $\mathbf{M}_{blue}$ (open circles), $\mathbf{M}_{green}$ (solid circles) and $\mathbf{M}_{red}$ (open triangles) in 10^{-5} M THF solution. Bands corresponding to π–π* and n–π* transitions are indicated on the spectra of $\mathbf{M}_{azo}$. (b) Absorbance spectra of terpolymers $\mathbf{TP}_{blue}$ (solid line), $\mathbf{TP}_{green}$ (dashed line) and $\mathbf{TP}_{red}$ (dotted line) in THF solution.

3.2. Synthesis, characterisation and optical properties of the polymers in solution

The general compositions and chemical structures of the synthesised polymers are collected in Scheme 1. The polymers were prepared by free-radical polymerisation in solution using DMF as the solvent and AIBN as the initiator. The physical characterisation was undertaken by IR, ^{1}H NMR, UV–vis spectroscopy and GPC, and the data are consistent with the expected structures. The reaction conditions were chosen taking into account results published for related copolymers [14]. These results claim that the retarding polymerisation effect of the azobenzene group is restricted in DMF, yielding polymeric systems with a composition that is in good agreement with the monomeric feed ratio.

The consumption of the monomeric feed mixture was controlled by monitoring the progress of the reaction by TLC. The final reaction conditions and purification procedures are collected in Table 2. For the preparation of $\mathbf{CP}_1$, 1% (weight ratio) AIBN was used and the polymer was isolated after a reaction time of 36 h. The composition of the copolymer $\mathbf{CP}_1$ was determined by ^{1}H NMR spectroscopy and was consistent with the feed composition.

Table 2
Composition of the synthesised polymers, polymerisation conditions and yields for the synthesised copolymers

Polymer	Composition (molar ratio)	Reaction time	Yield (%)	Purification
CP$_1$	**M**$_{am}$/**M**$_{azo}$ 75:25[a]	36 h	48	CH_2Cl_2 /EtOH
TP$_{blue}$	**M**$_{am}$/**M**$_{azo}$/**M**$_{blue}$ 70:15:15	4 days[b]	45	CH_2Cl_2 /EtOH
TP$_{green}$	**M**$_{am}$/**M**$_{azo}$/**M**$_{green}$[c] 70:15:15	6 days[d]	37	CH_2Cl_2/hexane
TP$_{red}$	**M**$_{am}$/**M**$_{azo}$/**M**$_{red}$[c] 70:15:15	5 days[d]	70	CH_2Cl_2 /EtOH

[a] Actual monomeric composition determined by ^{1}H NMR was 73:27.
[b] 3% of AIBN was used.
[c] The percentage of the luminescent comonomer (green or red) calculated by UV–vis was approximately 14%.
[d] 5% of AIBN was used.

In the case of the terpolymers, additional amounts of AIBN and prolonged reaction times were required in order to ensure complete reaction of the monomers. An additional 1% of AIBN was added every 24 h up to a final total amount of 3–5%. Due to the diversity of monomers, the final compositions of the terpolymers may differ slightly from that of the monomeric feed mixture. Determination of the actual composition by ^{1}H NMR spectroscopy was not possible because of signal overlap, which prevented accurate integration of the signals.

The UV/vis spectra were also complex due to overlap of the absorption bands (Fig. 1(b)). However, the absorption band at longer wavelengths in the case of **TP**$_{green}$ and **TP**$_{red}$ (474 and 445 nm, respectively) is only due to the absorption of the respective dye units. A correlation was established between the absorbance of the **M**$_{green}$ and **M**$_{red}$ monomers in solution and that of the terpolymers and this enabled the content of the dye units in the terpolymers to be estimated as ca. 14%, which is close to the theoretical value (15%). This implies that the polymeric composition must be similar to the monomeric feed composition.

The presence of the dye monomer in the polymeric systems was also qualitatively verified by studying luminescent properties. Emission spectra of the terpolymers were recorded in approximately 10^{-6} M THF by excitation at the maximum of the lowest energy absorption band. The results are collected in Table 3. The emission wavelengths are in accordance with that of the corresponding dye monomers in solution.

3.3. Thermal properties of the polymers

The thermal behaviour of the synthesised polymers was investigated by optical microscopy, DSC and TGA, and the results are collected in Table 3. The decomposition temperatures determined by thermogravimetric analysis were above 300 °C, demonstrating that the polymers have a good thermal stability.

In order to determine the transition temperatures and associated enthalpies by DSC, the copolymers were first heated to the isotropic state and then cooled to below 0 °C at a controlled rate. Data are given for the second heating scan. It was established by optical microscopy that all of the polymers have stable enantiotropic liquid crystalline phases.

After **CP**$_1$ had been heated above the clearing temperature and subsequently cooled, the copolymer was obtained as an amorphous glass with a T_g value of 59 °C. The polymer displays a SmA mesophase. This observation is consistent with the smectogenic tendency of related azobenzene/benzanilide-based liquid crystal polymers [14].

The thermal behaviour of **TP**$_{blue}$ and **TP**$_{red}$ is similar to that of **CP**$_1$. These compounds also show a SmA phase, which was identified from the typical fan texture viewed under crossed polarisers by optical microscopy. The incorporation of a third comonomer gives rise to a decrease in the T_g and clearing points (T_i) and broader transition peaks in the DSC curves. In addition, the DSC curves of **TP**$_{blue}$ and **TP**$_{red}$ show a higher tendency to crystallisation than the parent system **CP**$_1$. Indeed, on heating the sample a

Table 3
Optical properties in solution, thermal stability and thermal transitions of the polymers

Polymer	Optical properties[a]		Thermal properties[b]					
	λ_{max} (nm)	λ_{em} (nm)	TGA (°C)	DTGA (°C)	T_g (°C)	T_m (°C) (ΔH (kJ/mol))	T_i (°C) (ΔH (kJ/mol))	Mesophase
CP$_1$	280, 365		355	405	59		179 (3.7)	Smectic A
TP$_{blue}$	283, 350[sh]	438	313	355, 397	39[c]	108 (1.5)	135 (2.4)	Smectic A
TP$_{green}$	273, 453, 475	493, 524	343	401	58		97 (0.2)	Nematic
TP$_{red}$	286, 375, 445	603	338	394	38[c]	102 (1.1)	136 (1.3)	Smectic A

[a] Spectra were recorded in approximately 10^{-6} M solutions in THF. Values given in nm.
[b] TGA in °C, onset of the weight loss in thermogravimetric analysis; DTGA in °C, derivative thermogravimetric analysis; T_g in °C, glass transition temperature; T_m in °C, melting temperature; ΔH in kJ/mol of theoretical repeating unit: melting enthalpy; T_i in °C, isotropization temperature.
[c] Slow cold crystallization process above the T_g.

slow crystallisation process was detected above the T_g. The crystalline fraction slowly melted just above 100 °C.

In this context, $\mathbf{TP}_{green}$ shows characteristic behaviour that is certainly due to the molecular structure of the anthracene monomer, which is less rod-like in structure than the other monomers. In this case, the mesophase was identified as nematic and this was only stable over a narrow temperature range.

3.4. Photochemical stability of the dyes

A high photochemical stability for a dye is a prerequisite for technical applications. Therefore, the photostability of dyes $\mathbf{D}_{blue}$, $\mathbf{D}_{green}$ and $\mathbf{D}_{red}$ in a PMMA matrix was tested as a model for the terpolymers containing the related chromophores.

In general, push–pull substituted benzoxazoles show a quite high light-stability [20]. In contrast to the benzoxazoles, stilbene derivatives are highly photosensitive and can undergo *E*/*Z* photoisomerisation, [2+2] photocycloaddition and photocyclisation of the *Z* isomer to give a dihydrophenanthrene, which is followed by the irreversible oxidation to the corresponding phenanthrene. However, the formation of phenanthrene can be restricted by a strong push–pull substitution and the use of stiff matrixes [21]. Anthracene derivatives are known to undergo photooxidation and [4+4] photocycloaddition in the 9 and 10 positions. In addition, the photodegradation of $\mathbf{D}_{green}$ could be more complicated due to the presence of two triple bonds, which can undergo additional photoreactions.

A photodegradation level of 10% in the case of $\mathbf{D}_{blue}$ requires the absorption of an energy dose of about 47 J/cm^2 (see Section 2.4). The required dose for the degradation of $\mathbf{D}_{red}$ is 6.4 J/cm^2, which indicates a lower stability compared to $\mathbf{D}_{blue}$. Nevertheless, the stability is about one order of magnitude higher compared to the unsubstituted or donor–donor substituted stilbenes. $\mathbf{D}_{green}$ shows the lowest stability because an absorption dose of only 0.55 J/cm^2 is required for the same level of degradation. It is expected that the degradation of $\mathbf{D}_{green}$ will mainly be caused by the photooxidation of the anthracene in the 9 and 10 positions. In order to reduce the influence of oxygen, the poly(methyl methacrylate) (PMMA) film containing $\mathbf{D}_{green}$ was covered with a thin film of poly(vinylalcohol) (PVA). The PVA top layer protects the dye from oxygen and this significantly enhances the photostability by a factor of 22 (Fig. 2). In this case 10% degradation required the absorption of 12.3 J/cm^2.

3.5. Photophysical studies

The three dyes show strong emissions in both THF and PMMA films upon excitation at 335 nm in the case of $\mathbf{D}_{blue}$ and at 450 nm for $\mathbf{D}_{green}$ and $\mathbf{D}_{red}\mathbf{D}_{red}$ (Fig. 3). However, comparing the emission intensity with that of the terpolymers either in THF or as spin-coated films shows that a strong quenching effect occurs.

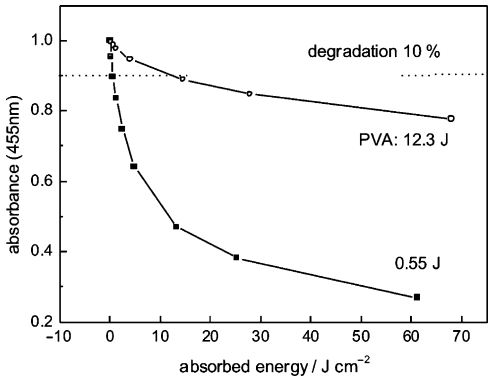

Fig. 2. Photostability of $\mathbf{D}_{green}$ upon irradiation at 436 nm in a non-protected PMMA film and a film covered with a PVA-top-layer detected at the maximum of the absorbance by UV/vis spectroscopy.

The quenching efficiency was determined by comparing the emission intensity of the dye-containing PMMA films with that of the related terpolymers using comparable absorption values at the excitation wavelength. It is estimated that approximately 95–99% of the emission is quenched in solution. The fluorescence of the spin-coated terpolymer films is quenched by almost 100%.

Comparable quenching behaviour is observed in films of the copolymer $\mathbf{CP}_1$ doped with the related dyes in a weight ratio of approximately 5:1. The emission of the fluorophores $\mathbf{D}_{green}$ and $\mathbf{D}_{red}$ was hardly detected and showed a bathochromic shift compared to dye-containing PMMA films.

There are several different photophysical processes that could be responsible for fluorescence quenching [19]. Recent papers report that fluorescence quenching of naphthalene and dansyl luminophores observed in the presence of covalently attached *trans*-azobenzene might occur through energy transfer as well as electron transfer [22]. Energy transfer quenching by the Förster-type mechanism does not require any interaction between the donor and the acceptor and can occur at distances up to 80–100 Å. However, such a process depends on the overlap

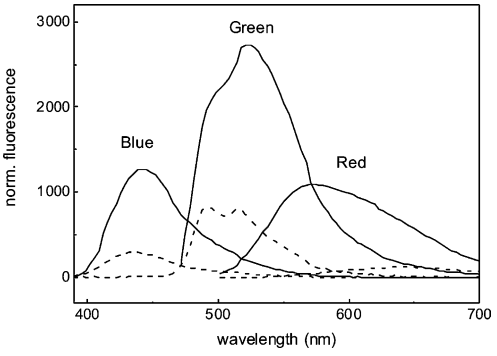

Fig. 3. Fluorescence spectra for $\mathbf{D}_{blue}$ (exc 335 nm), $\mathbf{D}_{green}$ (exc 450 nm) and $\mathbf{D}_{red}$ (exc 450 nm) in PMMA (solid lines) and the related terpolymers in THF (dashed lines). Curves have been normalized on the absorption value at λ_{max} of 0.9. The intensity of the emission of the terpolymers is multiplied by a factor of 5.

integral between the fluorescence of the donor and the absorption of the acceptor. This mechanism could explain the fluorescence quenching of the benzoxazole-containing polymer. For this reason, the emission of the benzoxazole was measured in terms of its dependence on the azobenzene concentration using THF solutions of $\mathbf{D}_{blue}$ in the presence of varying amounts of the copolymer $\mathbf{CP}_1$.

The results are represented as a Stern–Volmer plot in Fig. 4. The ratio of the fluorescence intensities I_0/I is greater than 1; I_0 is the intensity of the fluorescence without azobenzene and I in the presence of azobenzene. The linear slope of the Stern–Volmer plot shows the proportional decrease in the fluorescence of $\mathbf{D}_{blue}$ upon increasing the azobenzene concentration. Extrapolation of I_0/I to 2 in Fig. 4 and the use of Eq. (2) [23] allowed the average distance to be calculated between the energy donor and acceptor, R_0, for which 50% of the emission is quenched. The calculated value is $R_0 = 82 \pm 5$ Å.

$$R_0 = \frac{7.35}{\sqrt[3]{[\text{azobenzene}]_{I/I_0=2}}} \quad (2)$$

As stated above, the absorbance of the *E* isomeric form of the azobenzene is characterised by the π–π* transition at around 360 nm and the weak symmetry forbidden n–π* transition at 450 nm. Very recently, we have shown that the same azobenzene moiety of $\mathbf{M}_{azo}$ also undergoes photoisomerisation and photoorientation upon irradiation at 633 and 488 nm [24–26]. This is remarkable because the absorption coefficient is very small at these wavelengths. In contrast to the *E* isomer, the n–π* transition of the *Z* isomer is not symmetry forbidden and, for this reason, it has a slightly larger absorption coefficient around 450 nm. If the azobenzene moiety, either the *E* or the *Z* form, is excited directly via its absorbance or indirectly by energy transfer, a wavelength-dependent steady state between the two isomers should be established.

Comparison of the absorption and emission spectra of the $\mathbf{M}_{blue}$ monomer with the absorption spectra of the $\mathbf{M}_{azo}$ monomer shows that at 336 nm, which is the excitation wavelength of $\mathbf{M}_{blue}$, the two monomers have comparable absorption coefficients ($\varepsilon_{Mblue} = 16{,}461$ L/(mol cm) and $\varepsilon_{Mazo} = 15{,}800$ cm/M). This means that, at this wavelength and in a 1:1 molar ratio mixture of the two chromophores, about 45–50% of the light is absorbed by the azobenzene moiety, which would then undergo *E*/*Z* photoisomerisation. In addition to this, the $\mathbf{M}_{blue}$ emission overlaps the π–π* and n–π* absorption bands of the azobenzene. The quenching of the fluorescence of $\mathbf{M}_{blue}$ therefore seems to be caused by an energy transfer process that sensitises the *Z*/*E* photoisomerisation process of the *Z*-azobenzene, as proposed for similar bichromophoric compounds.

From an energetic point of view, quenching by the Förster transfer mechanism is only probable for the blue dye and cannot explain the quenching of the green and red emitting dyes [27] due to the small absorption of the azobenzene at the emission wavelengths of these dyes. Comparison of the fluorescence quenching of the dye moiety in $\mathbf{TP}_{green}$ and the related monomers in THF indicates that the quenching efficiency in the terpolymer is higher than that of the dissolved monomers in the same proportion (Fig. 5).

The reason for the higher quenching efficiency could be associated with the higher local concentration of azobenzene around the anthracene dye within the polymeric backbone compared to the molecular monomers in solution. The shorter distances between chromophores could give rise to specific intermolecular interactions that require molecular contact. In this case, quenching of the emission by an oxidative or reductive electron transfer process is possible [28,29]. This mechanism does not depend on the overlap of dye fluorescence with the azobenzene absorption but on the oxidation–reduction properties of chromophores.

Quenching by electron transfer can be either oxidative or reductive depending on the reductive or oxidising nature of the excited state fluorophore. For an oxidative electron transfer the feasibility of the process is given by Eq. (3) [19].

$$\Delta G \approx \left[E^0\left(\frac{A^+}{A}\right) - E^0\left(\frac{B}{B^-}\right)\right] - E_{00}A^* \quad (3)$$

where ΔG is the free energy of the quenching process in *V*, E^0 are the standard potentials of the ground state couples involved in the process, with A being the fluorophore and B

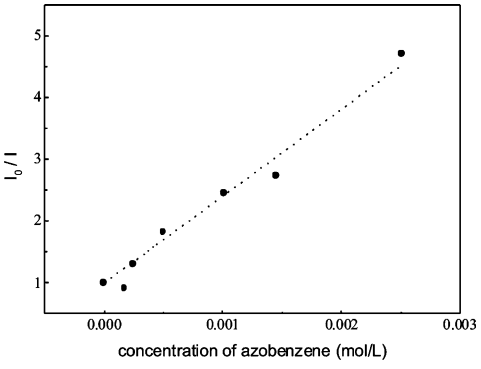

Fig. 4. Stern–Volmer plot of the fluorescence quenching of $\mathbf{D}_{blue}$ in THF at different azobenzene concentrations.

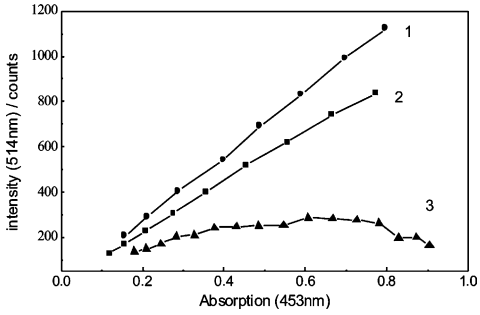

Fig. 5. Fluorescence of (1) $\mathbf{M}_{green}$, (2) a combination of $\mathbf{M}_{am}$, $\mathbf{M}_{azo}$ and $\mathbf{M}_{green}$ in 0.70:0.15:0.15 molar ratio, and (3) $\mathbf{TP}_{green}$ in THF at different absorbance values.

the $\mathbf{M}_{azo}$ quencher molecule, and E_{00}A* the spectroscopic energy of the excited state calculated from the onset of the emission peak in eV [30].

In order to examine the probability of such electron transfer processes, cyclic voltammetry measurements were carried out to determine the reduction and oxidation potentials of $\mathbf{M}_{azo}$ and the dye comonomers (Table 4).

The azobenzene is relatively difficult to oxidise and reduce (Fig. 6(a)). The voltammogram of $\mathbf{M}_{azo}$ shows an irreversible oxidation peak at +1.86 V. The reduction wave shows two peaks. The first one corresponds to a reversible reduction process with a half-wave reduction potential of −1.13 V. The voltammogram shows a second irreversible reduction process with a measured reduction peak potential at −1.60 V.

In relation to the fluorophores, $\mathbf{M}_{blue}$ did not show any oxidation process at positive potentials from 0 to +2 V. The monomer shows a reduction wave with good reversibility at a half wave potential of −1.57 V. The voltammogram of $\mathbf{M}_{green}$ at a positive potential shows one first irreversible oxidation wave at a peak potential of +1.20 V and a quasi-reversible oxidation wave at a peak potential of +1.50 V. In terms of negative potential values, a quasi-reversible reduction wave was observed at a half-wave potential of −1.32 V (Fig. 6(b)). Finally, $\mathbf{M}_{red}$ shows an irreversible oxidation process at a peak potential of +0.83 V. At negative voltages, a reversible reduction is observed at a half-wave potential of −1.20 V.

Therefore, on the basis of the excited state energy and electrochemical data listed in Table 4, electron transfer does not appear to be a possible mechanism of fluorescence quenching for $\mathbf{TP}_{blue}$, as both the reductive and oxidative processes are endergonic. However, we postulate that quenching may occur by electron transfer for $\mathbf{TP}_{green}$ and $\mathbf{TP}_{red}$ as oxidative electron quenching of the excited state of the fluorophore was found to be exergonic for $\mathbf{M}_{green}$ (ΔG is ca. −0.29 eV) and $\mathbf{M}_{red}$ (ΔG ca. −0.33).

Table 4
Oxidation and reduction potentials and energy of the excitated states of the azo and fluorescent monomers

Monomer	E_0 (V)[a]	E_{red} (V)[b]	E_{00} (eV)
$\mathbf{M}_{azo}$	+1.86	−1.13, −1.60[c]	
$\mathbf{M}_{blue}$	[d]	−1.57	3.27
$\mathbf{M}_{green}$	+1.20, +1.50	−1.32	2.62
$\mathbf{M}_{red}$	+0.83	−1.20	2.30

E_{ox} is given from the oxidation cyclic voltammogram and E_{red} from the reduction cyclic voltammogram. For reversible process values are given as $E_{1/2}$ (half-wave potential) calculated as the midpoint between the cathodic and anodic peaks. For irreversible processes values are given as E_p (peak potential) as the maximum of the corresponding peak; Zero–zero spectroscopic energy of the excited state E_{00}.

[a] Oxidation potentials are given as E_p because the oxidation processes of all monomers were irreversible.

[b] Reduction potentials were given as $E_{1/2}$ unless otherwise stated.

[c] E_p value is given because this second reduction process was irreversible.

[d] No oxidation process was observed up to 2 V.

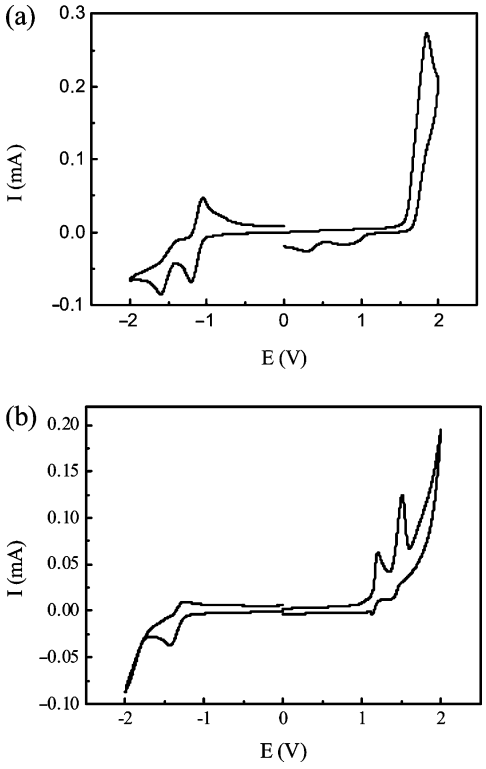

Fig. 6. (a) Cyclic voltammogram of $\mathbf{M}_{azo}$, oxidation in CH_2Cl_2 and reduction in THF. (b) Cyclic voltammogram of $\mathbf{M}_{green}$ in THF solution. The voltammograms were recorded at a scan rate of 0.05 V/s.

4. Conclusions

Multifunctionalised polymers were synthesised in which three different side groups introduce liquid crystalline, photochromic and specific absorption and emission properties. The mutual interactions of the side groups were investigated with respect to these properties and functions. The photochromic properties of the azobenzene are unchanged but the incorporation of the different dyes results in a change in the absorption. However, the fluorescence of the dyes is strongly quenched in the presence of the azobenzene moiety. For this reason all applications based on absorption are favoured but all applications based on emission become impossible. Therefore, the creation of dichroic absorptive films by light-orienting procedures is a potential application for these polymers. High light stability is a prerequisite for the orientation of the terpolymers by photoorientation to generate anisotropic films. In this way, the photochromism of the azobenzenes can be used, but the strong filter effect of the dyes requires excitation of the azobenzene moieties at wavelengths at which the dyes have a spectral gap. The light stability of the dyes under investigation is higher than for other dyes of the same family and, furthermore, the photostability of the anthracene derivative is significantly increased by covering the sample with a PVA top-layer in order to exclude the influence of oxygen. As part of our research program, a careful study of the processing conditions for films of these terpolymers—

including irradiation wavelengths, irradiation time, annealing temperatures and the generation of anisotropy—have been the object of a recent publication [31].

Acknowledgements

This work was supported by the EEC Brite/Euram project BE97-4210, the CICYT-FEDER Spanish projects MAT 2002-04118-C02-01 and MAT 2003-07806-C02-01, the Government of Aragon and the Programa Ramón y Cajal (MCyT-MEC, Spain). We thank Prof J. Garín (University of Zaragoza) and his research group for assistance with the cyclic voltammetry measurements.

References

[1] Kelly SM. Flat panel displays: Advanced organic materials. In: Connor JA, editor. RSC materials monographs. Cambridge: Royal Society of Chemistry; 2000.
[2] Weder C, Sarwa C, Montali A, Bastiaansen C, Smith P. Science 1998; 279:835–7.
[3] Kumar GS, Neckers DC. Chem Rev 1989;89:1915–25.
[4] Shibaev V, editor. Polymers as electrooptical and photooptical active media. Heidelberg: Springer; 1996.
[5] Natansohn A, Rochon P. Chem Rev 2002;102:4139–75.
[6] Läsker L, Fischer Th, Stumpe J, Kostromin S, Ivanov S, Shibaev V, et al. Mol Cryst Liq Cryst 1994;252:293–302.
[7] Läsker L, Fischer Th, Stumpe J, Kostromin S, Ivanov S, Shibaev V, et al. Mol Cryst Liq Cryst 1994;246:347–50.
[8] Läsker L, Fischer Th, Stumpe J, Kostromin S, Ivanov S, Shibaev V, et al. Mol Cryst Liq Cryst 1995;261:371–81.
[9] Stumpe J, Läsker L, Fischer Th, Rutloh M, Kostromin S, Ruhmann R. Thin Solid Films 1996;285:252–6.
[10] Rosenhauer R, Fischer Th, Czapla S, Stumpe J, Viñuales A, Piñol M. Mol Cryst Liq Cryst 2001;364:295–304.
[11] Shibaev V, Bobrovsky A, Boiko N. Prog Polym Sci 2003;28:729–836.
[12] Bobrovsky A, Boiko N, Shibaev V. J Mater Chem 2000;10:1075–81.
[13] Ruhmann R, Zschuppe V, Dittmer M, Wolff D. Makromol Chem 1992;193:3073–82.
[14] Czapla S, Ruhmann R, Rübner J, Zschuppe V, Wolff D. Makromol Chem 1993;194:243–50.
[15] Robello DR. J Polym Sci, Part A: Polym Chem 1990;28:1–13.
[16] Gimenez R, Piñol M, Serrano JL. Chem Mater 2004;16:1377–83.
[17] The absorbed energy dose is changed by the loss of the dye absorbance during the irradiation. For this reason the mean absorbance between every irradiation step was used for the calculation.
[18] Lucht S, Stumpe JJ. Luminescence 2000;91:203–14.
[19] Valeur B. Molecular fluorescence. Weinheim: Wiley; 2002.
[20] Unpublished results.
[21] Fuhrmann Th, Kunze M, Lieker I, Stracke A, Wendorff JH. In: Mohlmann GR, editor. Proceedings of SPIE NLO properties of organic materials IX, vol. 2852, 1996. p. 42–52.
[22] Vögtle F, Gorka M, Hesse R, Ceroni P, Maestri M, Balzani V. Photochem Photobiol Sci 2002;1:45–51. Ceroni P, Laghi I, Maestri M, Balzani V, Gestermann S, Gorka M, et al. J Chem 2002; 26:66–75.
[23] Eq. (2)is used on the assumption that all components are molecularly solved and self-quenching of the dyes can be neglected. I_0/I equal 2 means the concentration of acceptor or quencher molecules that reduce the emission to half of the value measured in absence of the quencher.
[24] Stumpe J, Fischer Th, Rutloh M, Rosenhauer R, Meier JG. In: Khoo IC, editor. Proceedings of SPIE liquid crystals III, vol. 3800, 1999. p. 150–63.
[25] Rutloh M, Stumpe J. J Inform Rec 2000;25:39–46.
[26] Kempe Ch, Rutloh M, Stumpe J. J Phys: Condens Matter 2003;15: S813–S23.
[27] Rosenhauer R, Fischer Th, Stumpe J, Gimenez R, Pinol M, Serrano JL. In: Khoo IC, editor. Proceedings of SPIE liquid crystals VI, vol. 4799, 2002. p. 121–35.
[28] Schmälzlin E, Bitterer U, Langhals H, Bräuchle Ch, Meerholz K. Chem Phys 1999;245:73–8.
[29] Sander T, Löhmannsröben H-G, Langhals H. J Photochem Photobiol A Chem 1995;86:103–8.
[30] A similar equation can be written for a photoinduced reductive electron transfer.
[31] Rosenhauer R, Fischer Th, Stumpe J, Gimenez R, Piñol M, Serrano JL, et al. Macromolecules 2005;38:2213–22.